Fluorescence blinking in MoS2 atomic layers by single photon energy transfer

Mai He
School of Physics and Electronics, Hunan University
Cuihuan Ge
School of Physics and Electronics, Hunan University
Kai Braun
University of Tübingen
Lanyu Huang
School of Physics and Electronics, Hunan University
Xin Yang
Key Laboratory for Micro-Nano Physics and Technology of Hunan Province, College of Materials Science and Engineering, Hunan University
Hepeng Zhao
School of Physics and Electronics, Hunan University
Alfred Meixner
University of Tubingen https://orcid.org/0000-0002-0187-2906
Xiao Wang (xiao_wang@hnu.edu.cn)
Hunan University https://orcid.org/0000-0002-2973-8215
Anlian Pan
Hunan University https://orcid.org/0000-0003-3335-3067

Article

Keywords:

Posted Date: December 2nd, 2021

DOI: https://doi.org/10.21203/rs.3.rs-1092426/v1

Fluorescence blinking in MoS_2 atomic layers by single photon energy transfer

Mai He[1], Cuihuan Ge[1], Kai Braun[3], Lanyu Huang[1], Xin Yang[2], Hepeng Zhao[1], Alfred J. Meixner[3], Xiao Wang[1], Anlian Pan[2*]*

[1]School of Physics and Electronics, Hunan University, Changsha 410082, China

[2]Key Laboratory for Micro-Nano Physics and Technology of Hunan Province, College of Materials Science and Engineering, Hunan University, Changsha 410082, China

[3]Institute of Physical and Theoretical Chemistry and LISA+, University of Tübingen, Auf der Morgenstelle 18, 72076, Tübingen, Germany

*Email: xiao_wang@hnu.edu.cn; anlian.pan@hnu.edu.cn

Abstract: The quantum optical phenomena, such as single photon emission, in two-dimensional (2D) transition metal dichalcogenides (TMDCs) have triggered extensive researches on 2D material-based quantum optics and devices. By far, most reported quantum optical emissions in TMDCs are based on atomic defects in the material or the local confinement of excitons by introducing local stain or potential. In contrast, energy transfer between two materials could also manipulate the photon emission behaviors in materials, even at the single photon level. Along with the single-photon emission nature of zero-dimensional (0D) quantum dots (QDs) at room temperature, constructing a 0D-2D hybrid heterostructure may provide an effective way to regulate the quantum states related optical emissions of TMDCs. Here, we report on fluorescence blinking, a quantum phenomenon, from MoS_2 atomic layers in QD/ MoS_2 heterostructure at room temperature. We demonstrate the single-photon nature of the QDs in heterostructures by second-order photon correlation measurements. Based on the transient PL spectroscopy and PL time trajectories, we attribute the fluorescence blinking behavior in MoS_2 to the single photon energy transfer from QD to MoS_2. Our work opens the possibility to achieve correlated quantum emitters in TMDCs at room temperature by controlling the energy transfer between QD and TMDCs.

Introduction

2D TMDCs have received extensive attention for both fundamental research[1-5] and photonic applications[6-11] due to the large exciton binding energy[5,12], tunable bandgap covering from visible to near infrared [13,14], and van der Waals (vdW) integration with other materials[15-17]. Furthermore, the 2D quantum confinement in atomic layer thin

TMDCs brings unique quantum effects[18-20], which makes them excellent candidates for device applications in quantum information. In recent years, a large number of researchers have been devoted to studying quantum optical properties of 2D materials. For instance, single atom defects in 2D materials have been demonstrated to act as single photon emitters upon photon excitation [21-24], which provide the essential element for quantum communication and computing based on 2D materials. Besides, artificially constructed TMDCs layers by the introduction of nanobubble[25], wrinkles[26], nanometer-sized gold tips[27] or pattern arrays of nanopillars[28,29], have also been reported to behave as single photon sources in local strained areas due to the strain induced local confinement of excitons. These TMDCs materials provide a scalable platform for quantum photonic applications in a relatively controlled manner.

2D TMDCs can form the vdW heterostructure by vertically stacking two different TMDCs materials that provides unprecedented characteristics beyond single component[15,16]. Recently, unique optical quantum phenomena have also been demonstrated in TMDCs heterostructures[30,31]. Unlike the stable photoluminescence (PL) intensity emitted by TMDCs monolayer, the PL emission in $WS_2/MoSe_2$ heterostructures exhibits blinking behavior, and the fluorescence fluctuation of this system jumped between bright, neutral and dark states, owing to an intermittent interlayer carrier transfer process[30]. Lately, the single photon emission due to the interlayer excitons in $MoSe_2/WSe_2$ heterostructure was reported, which can be interpreted as the interlayer excitons were locally confined by the generated moiré potential in the heterostructure [31]. However, the twist angle in these heterostructures

needs to be precisely controlled to form an effective moiré potential and the single photon emission is observed at cryogenic temperature. In contrast to conventional 2D heterostructures, 0D-2D hybrid heterostructures consisting of quantum dots and TMDCs layers also provide an effective route to manipulate the photonic properties of 2D TMDCs[32], especially, along with the single photon emission nature of the 0D materials[33-36]. However, most of the previous studies on the 0D-2D heterostructures have focused on increasing the absorption of acceptor by improving energy transfer efficiency, including the regulation of the distance between the donor and the acceptor[37,38], the spectral overlap between the emission of the donor and absorption of the acceptor[38,39], the direction of the dipole[40], and the screening of the electric field from the acceptor[41,42]. The energy transfer on the single photon level in TMDCs is rarely studied. Hence, constructing 0D-2D heterostructures and exploring the interaction with single photon energy transfer could be an indispensable way to manipulate quantum states in TMDCs materials.

In this work, we constructed a hybrid heterostructure consisting of CdSe/ZnS core-shell QD and MoS_2 atomic layers to study the quantum states related optical emissions. The second-order photon correlation measurements indicate that the single-photon nature of the QDs in heterostructures still maintains after energy transfer with MoS_2. By studying transient PL and PL time trajectories of QD/monolayer-MoS_2 heterostructure, we found that the fluorescence blinking behavior of MoS_2 can be attributed to the intermittent energy transfer on the single photon level. Meanwhile, a less prominent blinking phenomenon of MoS_2 bilayer in QD/bilayer-MoS_2

heterostructure demonstrates that the change in energy transfer efficiency directly affects the variation of quantum states in MoS_2.

Results

Single photon emission of QD in QD/monolayer-MoS_2 heterostructure

Monodispersed QDs on cover glass were prepared by the spin-coating method. Exfoliated MoS_2 flakes were then transferred onto the QDs to form QD/MoS_2 heterostructures. Figure 1a shows the optical image of the heterostructures and Figure 1b shows the PL image of QDs in the same area. Compared to the pure QDs, a significant PL quenching in the QD/monolayer-MoS_2 heterostructure is observed, the area of which is marked with orange dashed lines in both Figure 1a and 1b. The magnified PL image (Fig. 1c) of the heterostructure area shows typical diffraction-limited emission patterns and demonstrates that the QDs are well monodispersed, which provides a perfect platform to study the interaction between a single QD and the monolayer MoS_2. The image of a single QD shows a typical photon blinking behavior with an intermittent appearance of dark strips (Fig. 1d), which can be ascribed to the dark states of the PL emission.

On account of the core-shell structure of QDs and long-chain organic molecules (oleic acid) surrounding the shell, the charge transfer process between QDs and MoS_2 is nearly impossible, since the spacing between the donor and acceptor for charge transfer is usually less than 1nm[43]. We attribute the quenching of the overall QDs PL in the heterostructures to the Förster resonance energy transfer (FRET) from QDs to MoS_2 (Fig. 1e). The QDs have the PL emission spectral profile (Supplementary Fig. 1) that

overlaps with the direct excitonic absorption peak of MoS_2 (Fig. 1h), which is an important condition for FRET[41]. Furthermore, the PL lifetime of QDs in heterostructures decreases obviously compared with that of pure QDs deposited on cover glass (Supplementary Fig. 2), which is also a crucial characteristic of FRET[44].

To investigate the variation of the single-photon nature of a single QD in this hybrid 0D-2D heterostructure, second-order photon correlation measurements $g^2(\tau)$ were performed at room temperature, under the excitation of a 405 nm laser source with both continuous wave (cw) and pulsed modes. When excited by the cw 405 nm laser, the $g^2(\tau)$ curves show a typical dip at time zero with $g^2(0) = 0.17$ for a single QD on cover glass (Fig. 1f), and $g^2(0) = 0.36$ for a QD in the heterostructure (Fig. 1g). When excited by the pulsed 405nm laser, we observed a largely reduced or nearly disappeared pulse peak at time zero in $g^2(\tau)$. We obtain $g^2(0) = 0.05$ for the pure QD (Fig. 1i) and $g^2(0) = 0.34$ for the QD in heterostructures (Fig. 1j). The fitting details of second-order photon correlation function are given in Supplementary Note 3. The enlarged $g^2(0)$ is due to the additional background noise caused by the fluorescence of MoS_2 in the heterostructure.[45] Nevertheless, all observed $g^2(0)$ values are less than 0.5, indicating that the single-photon nature of the single QD in the heterostructure still maintains.[46]

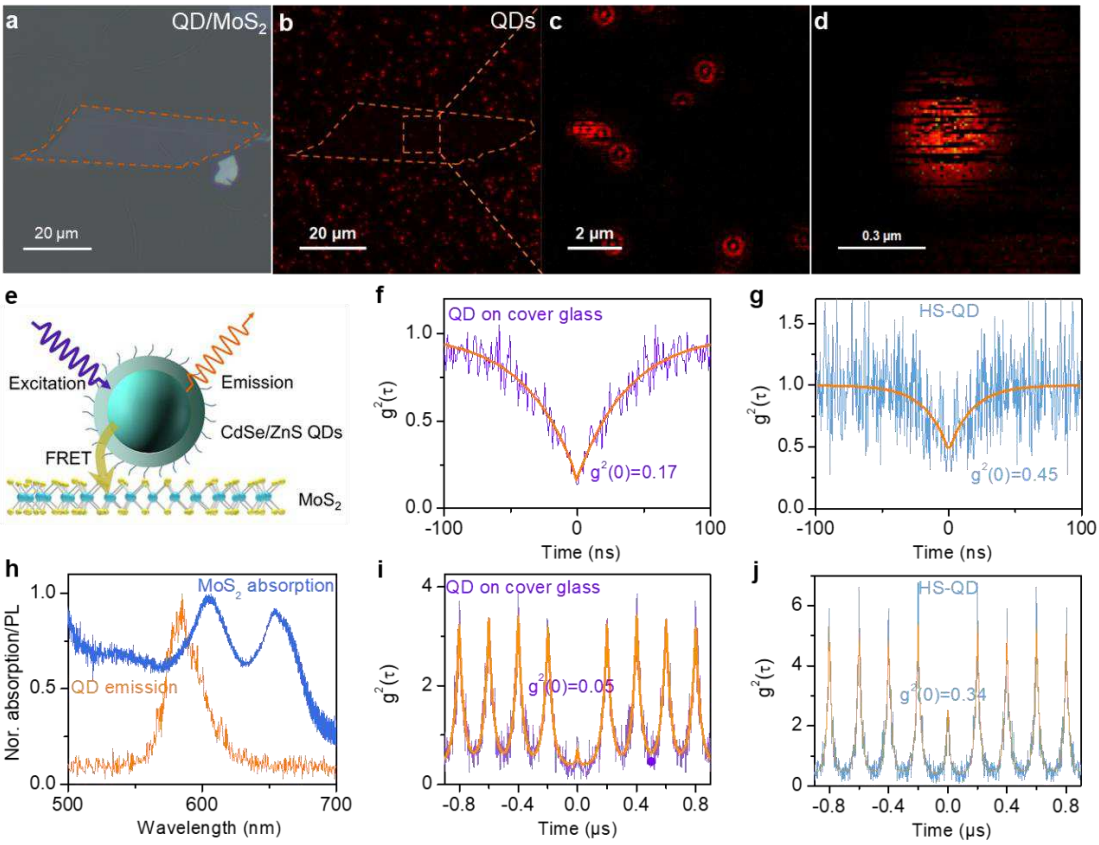

Fig. 1 Single photon emission of a single QD in QD/monolayer-MoS_2 heterostructure. a, Optical image of exfoliated MoS_2 monolayer on QD film. **b**, PL image of QDs, showing significant PL quenching for QDs in heterostructures vs QDs deposited on cover glass slides. **c**, Magnified PL image of the heterostructure area in **b**. **d**, PL image of a single quantum dot, showing a typical spatial resolution (about 240 nm). **e**, Schematic representation of FRET about CdSe/ZnS QDs/MoS_2 heterostructure. **h**, The overlap between the QD emission profile and the MoS_2 absorption profile. **f** and **i** are second-order correlation function curves obtained from a QD on cover glass slide excited by a 405 nm laser under cw mode and pulsed mode at room temperature, respectively. While **g** and **j** are second-order correlation function curves obtained from a QD in heterostructures. Orange curves represent fitted data obtained by an exponential decay function.

Fluorescence blinking in MoS_2 monolayer

To study the variations of quantum emission states from a single QD and MoS_2 in heterostructure, the PL intensity time trajectories from a single QD on the cover glass and in the QD/monolayer-MoS_2 heterostructure were recorded by time-correlated single photon counting (TCSPC) system (Fig. 2a and 2c). For both cases, we observe the typical PL emission blinking behavior. However, the occurrence of the low intensity emission from the QD in heterostructure is obviously increased (Fig. 2c). Accordingly, we plot the fluorescence intensity distributions and their bimodal Gaussian fitting in Figure 2b and 2d. Two peaks from the fitting data can be assigned to the bright state (B-state) and the dark state (D-state) of blinking. It can be seen from these statistics that the proportion of the B-state decreased while the proportion of the D-state increased for the QD in heterostructure. This observation agrees with the proposed energy transfer process between the QD and MoS_2 in the heterostructure, which makes the initial B-state of QD transit to the D-state.

Besides, we monitor the PL intensity time trajectories from the pure MoS_2 monolayer and the MoS_2 monolayer in heterostructure (HS-MoS_2) (Fig. 2e). Compared to the relatively stable fluorescence emission from pure MoS_2 monolayer (purple curve in Fig. 2e), the fluorescence emission of HS-MoS_2 shows obvious blinking behavior due to its interaction with a QD (blue curve in Fig. 2e). The fluorescence intensity distribution statistics in Figure 2f shows that the HS-MoS_2 has a wide distribution consisting of D-state and B-state, similar to the emission states of a QD. Considering the energy transfer process in heterostructure, when the excitation laser energy higher than the band gap of

154 the QD (donor), the energy of the excited electron-hole pair from the QD would transfer
155 to the MoS_2 monolayer (acceptor) in a non-radiative way[47]. As a result, the fluorescence
156 of the QD quenched and the fluorescence of the MoS_2 monolayer increased. Since the
157 single photon emission nature of QD, the energy transfer in this system occurs with the
158 association of the quantum states of the emission, leading to a typical blinking behavior
159 in MoS_2 monolayer. Therefore, we observe the fluorescence blinking in MoS_2
160 monolayer by the energy transfer from single QD on the single photon level.

161

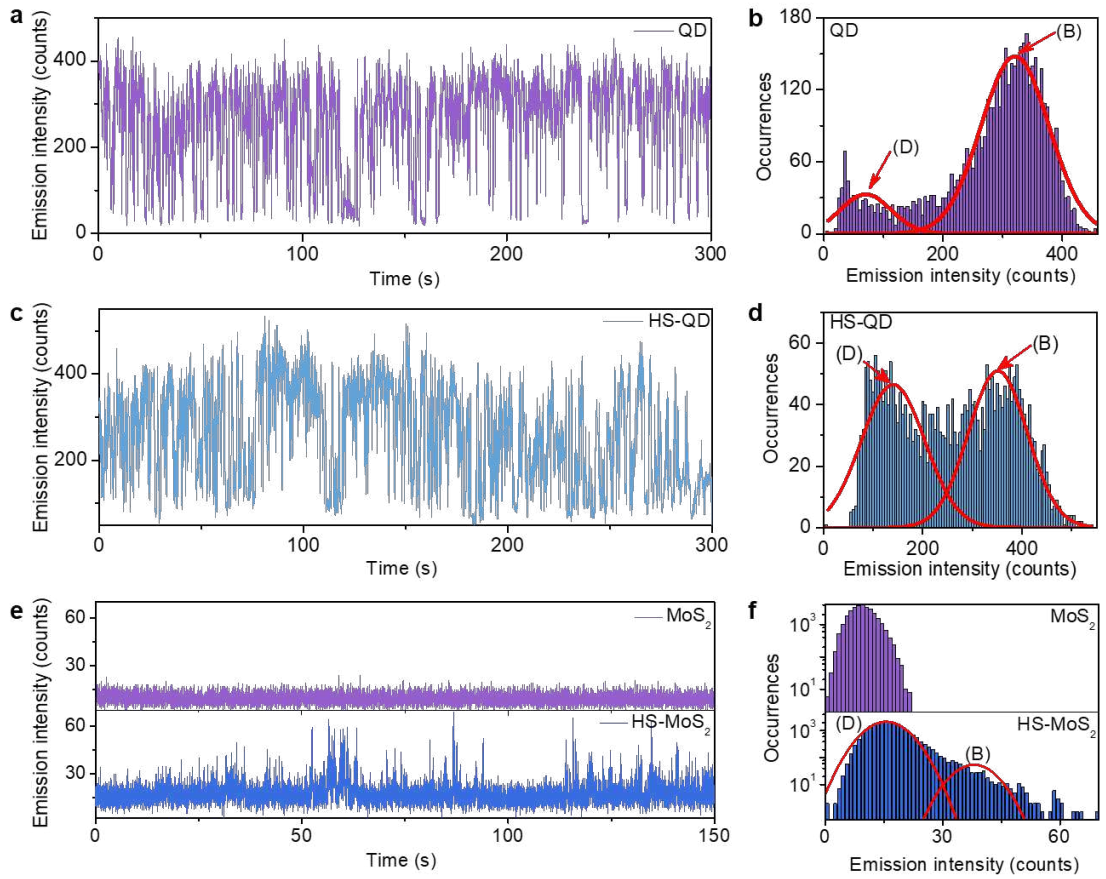

Fig. 2 Fluorescence Blinking from MoS_2 monolayer in a heterostructure. a, **c**, PL intensity time trajectories from a QD on a cover glass slide and a QD in a QD/MoS_2 heterostructure, respectively. **b**, **d**, Statistics of emission intensity from **a** and **c**, indicating that the B-state decreases and the D-state increases due to the interfacial interaction. **e**, PL intensity time trajectories from a pure MoS_2 monolayer (purple curve) and a MoS_2 monolayer in HS-MoS_2 (blue curve), show obvious variations in emission intensity. **f**, Statistics of emission intensity from **e**. Compared to pure MoS_2 monolayer, a broader range of emission intensity in HS-MoS_2 are observed.

Fluorescence cross-correlation of QD and MoS_2 in heterostructure

In order to further understand the origin of blinking behavior from the MoS_2 in heterostructure, we simultaneously detected the PL intensity time trajectories from the MoS_2 and the single QD at the same position of the heterostructure (Fig. 3a). The PL signals were selectively recorded by narrow band-pass filters with center wavelengths at 575 nm and 660 nm for QD and MoS_2, respectively (Supplementary Fig. 4). We observed typical blinking behavior from both QD and MoS_2. It is found that when the monolayer MoS_2 (blue dots in Fig. 3a) is in the B-state (stronger emission), the corresponding signal of QD (orange dots in Fig. 3a) is almost in the D-state. This negative correlation at certain time periods can be seen clearly in Figure 3b. The statistics of emission intensity extracted from Figure 3a is shown in Figure 3e and the three possible interactions (marked in Fig. 3e) between MoS_2 monolayer and QD are illustrated in Fig. 3c and 3d. When QD is in the B-state, if there is no energy transfer between QD and MoS_2, MoS_2 will maintain the original emission intensity and be in the D-state as we defined in the system (case I in Fig. 3c); While, if the energy transfer occurs between it and MoS_2 at this time, the fluorescence intensity of MoS_2 will be enhanced, leading to the B-state of MoS_2 (case II in Fig. 3d). When we hypothesize that the QD is in the D-state, energy transfer will not occur, and MoS_2 will be still in the D-state at this time, as indicated in case III in Figure 3e. Furthermore, we have also observed similar blinking behavior in other QD/MoS_2 hybrid heterostructures (Supplementary Fig. 5).

The PL lifetime from QD and MoS_2 during the time trajectory measurements can

also be extracted from the simultaneously recorded singles with the TCSPC system. Although the obtained lifetime shows fluctuations due to the short binning time and low photon number, the average lifetime of QD is about 5 ns (dark yellow dots in Fig. 3f) during this measurement, which is clearly distinct from the short lifetime (about 0.5 ns in average) of MoS_2 (blue dots in Fig. 3f). This observation excludes the crosstalk about the emission signal from QD and MoS_2 in two detection channels, further confirming the blinking is indeed from the emission of MoS_2. Meanwhile, the fluctuation with time could be also a consequence of the intermittent energy transfer from the QD to the MoS_2. Since the lifetime of pure MoS_2 monolayer over time is maintained as a relatively stable and almost uniform value at different excitation fluences (Supplementary Fig. 6), the lifetime fluctuation caused by instrument instability would be ruled out. In addition, we also counted the lifetime distribution of the two from Figure 3f. From this distribution, it is shown that while the MoS_2 has a long lifetime, the corresponding QD generally has a short lifetime (blue area in Fig. 3g), which also implies the existence of intermittent energy transfer.[44]

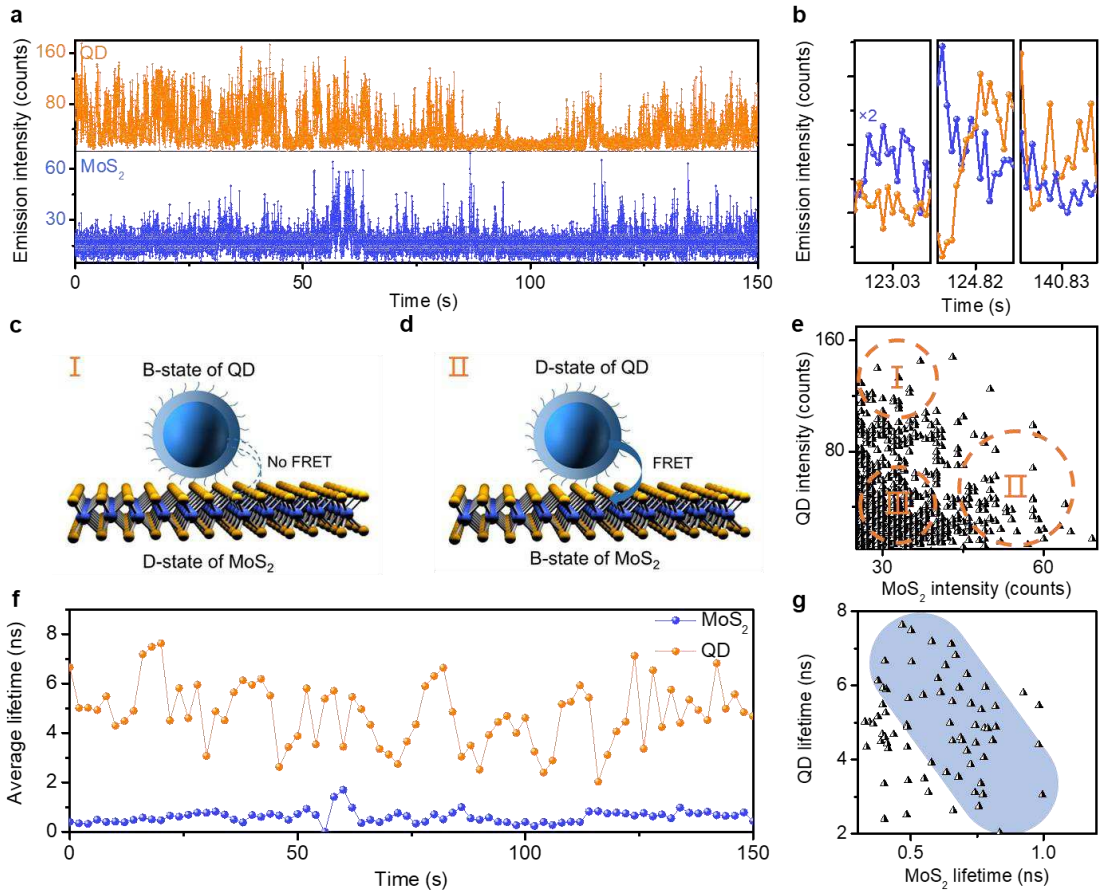

Fig. 3 Fluorescence cross-correlation of QD and MoS_2 monolayer in heterostructure. a, PL intensity time trajectories from QD (orange curve) and MoS_2 monolayer (blue curve) in QD/monolayer-MoS_2 heterostructure. The binning time is 10 ms. **b**, PL emission intensity extracted from **a** at certain time periods, revealing a distinct negative correlation. **c**, **d**, Schematic diagrams of fluorescence blinking behavior in MoS_2. Dotted arrow indicate no FRET in heterostructure. **e**, The emission intensity distribution of QD and MoS_2 monolayer extracted from **a**. The areas of three circles dotted lines represented the three cases of interaction between QD and MoS_2. **f**, Time trace of average lifetime from QD (orange curve) and MoS_2 monolayer (blue curve) in QD/monolayer-MoS_2 heterostructure. **g**, Lifetime distribution of QD and MoS_2 monolayer extracted from **f**.

Energy transfer and fluorescence blinking in QD/bilayer-MoS_2 heterostructure

We further investigate the interaction between a single QD and a bilayer MoS_2 under optical excitation. The QD/bilayer-MoS_2 heterostructure was obtained by transferring a mechanically exfoliated MoS_2 flake on a cover glass coated with QDs. The area of the heterostructure was marked by white dashed lines in the optical image (Fig. 4a). As MoS_2 changes from monolayer to bilayer, the screening of the electric field increases[41,42], so that the energy transfer efficiency between QDs and MoS_2 greatly decreases (Fig. 4c). To demonstrate the change of the energy transfer efficiency, we recorded the QDs PL lifetime image of QD/bilayer-MoS_2 (Fig. 4b) and QD/monolayer-MoS_2 heterostructures (Supplementary Fig. 2). Quantitatively, we perform statistics on the PL lifetime of QDs. Through Gaussian fitting, we found that the mean lifetime of QDs in QD/bilayer-MoS_2 heterostructures was about 7.28 ns (red curve in Fig. 4d), while the mean lifetime of QDs in QD/monolayer-MoS_2 heterostructures was about 2.18 ns (blue curve in Fig. 4d). Representative lifetime measurements of QD on the cover glass and in heterostructures are shown in Figure 4e. In addition, the energy transfer efficiency can be expressed as $\eta_{\mathrm{FRET}=1-\frac{\tau_{DA}}{\tau_D}}$, [38] where τ_{DA} and τ_D are the lifetimes of the QD in heterostructure and on cover glass, respectively. Using this formula, we obtain that the energy transfer efficiencies in QD/monolayer-MoS_2 and QD/bilayer-MoS_2 are 78.1% and 27.0%, respectively.

We also study the single-photon nature of the single QD in QD/bilayer-MoS_2 heterostructure (Fig. 4f). We obtain $g^2(0) = 0.26$ by fitting data (blue curve), which is a bit better than QD from MoS_2/QD hybrid heterostructure. This may be due to the fact

243 that, compared to the case for MoS_2 monolayer, MoS_2 bilayer is an indirect band gap
244 material [5] with a relatively weak fluorescence emission, which leads to a low
245 background noise in the second-order photon correlation measurement. Meanwhile, we
246 tested the PL intensity time trajectories from single QDs and MoS_2 bilayer (Fig. 4g)
247 and compared the intensity relations (Fig. 4h). The emission intensity of QD is still
248 negatively correlated with that of MoS_2 bilayer at certain time periods (blue area in Fig.
249 4h). The blinking behavior from MoS_2 bilayer in this heterostructure is clearly weaker
250 than that of MoS_2 in QD/monolayer-MoS_2 hybrid heterostructure (see the blue data in
251 Fig. 4g), which is consistent with the low energy transfer efficiency in this
252 heterostructure.
253

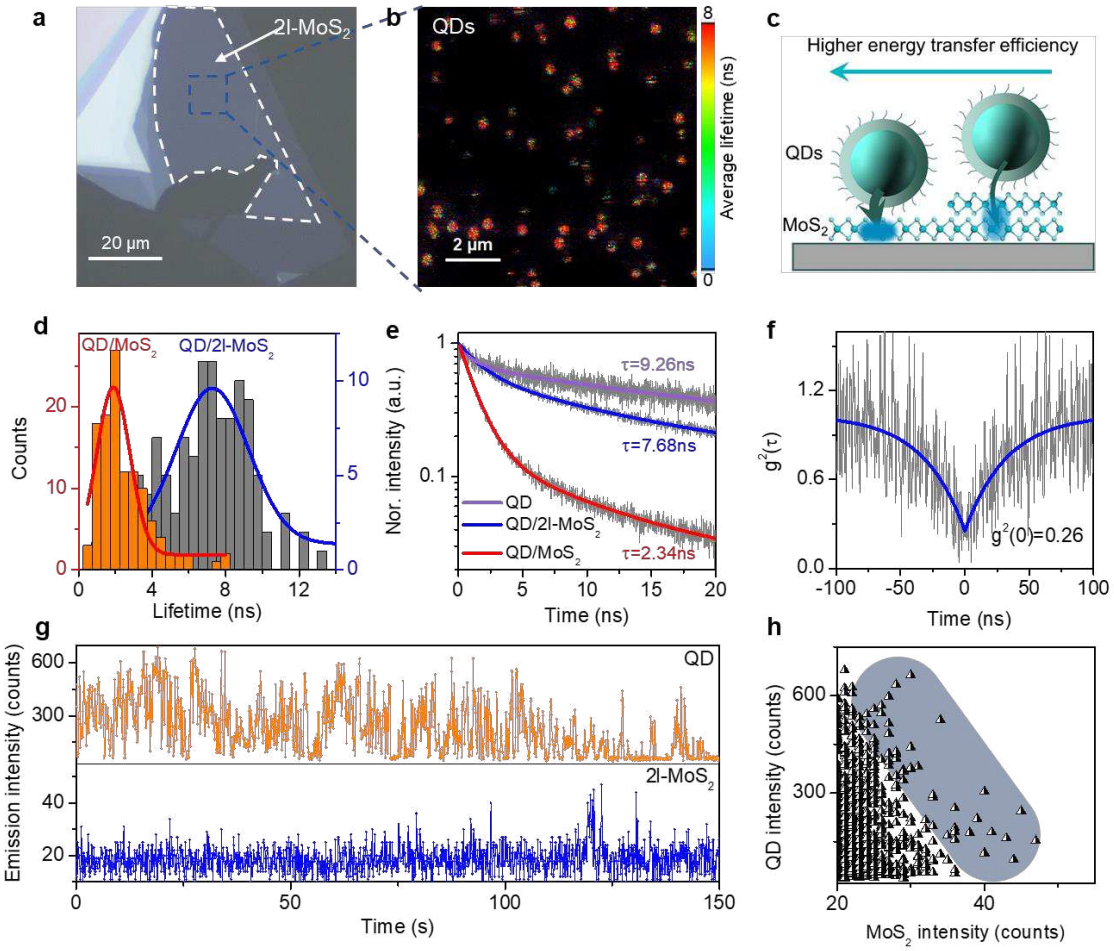

Fig. 4 Energy transfer and fluorescence blinking in QD/bilayer-MoS_2 heterostructure. a, Optical image of exfoliated MoS_2 flakes on a QD film. The white dashed lines show the area of the bilayer-MoS_2 (2l-MoS_2). **b**, PL lifetime image of QDs from the area in **a** marked with blue dashed lines. **c**, Schematic of energy transfer efficiency varying with the number of MoS_2 layers. **d**, Statistics of PL lifetime of QDs in QD/monolayer-MoS_2 (QD/MoS_2) and in QD/bilayer-MoS_2 (QD/2l-MoS_2) heterostructures. **e**, Representative PL decay curves from QD on cover glass, in QD/MoS_2 and QD/2l-MoS_2 heterostructures. **f**, Second-order correlation function curve obtained from a QD in QD/2l-MoS_2 heterostructure at room temperature. **g**, PL intensity time trajectories from QD (purple curve) and 2l-MoS_2 (blue curve) in QD/2l-MoS_2 heterostructure. Binning time is 100 ms. **h**, PL intensity distribution of QD and MoS_2 derived from **g**. The data in blue area indicates a negative correlation between these two intensities.

Discussion

In conclusion, we have demonstrated fluorescence blinking in MoS_2 monolayer and bilayer due to the single photon energy transfer from single CdSe/ZnS QDs. We investigated the second-order photon correlation measurements of QDs with and without the energy transfer process, demonstrating that the QDs in heterostructures still maintain the single-photon nature. By comparing the PL intensity time trajectories of the QDs on cover glass to that of the QDs in heterostructures, we find the proportion of the D-state in QDs from heterostructures is significantly increased due to the energy transfer. Meanwhile, the PL intensity time trajectories of MoS_2 in heterostructures show a fluorescence-blinking behavior similar to the emission states of QDs. With simultaneously recorded PL intensity time trajectories of QD and MoS_2 in heterostructure, a negative correlation between the two signals at certain time periods is observed, which further confirms that the fluorescence-blinking is due to the energy transfer between QD and MoS_2 on the single photon level. As the screening of the electric field effect of MoS_2 increases with the number of layers, we explore the interaction between QDs and MoS_2 bilayer. The statistics of PL lifetime of QDs in heterostructures demonstrate that the energy transfer efficiency is smaller in QD/bilayer-MoS_2 heterostructure compared to that from QD/monolayer-MoS_2. Consequently, we observe a less prominent fluorescence blinking behavior in bilayer MoS_2, which is consistent with the energy transfer efficiency. Our findings could contribute to a deeper understanding of the energy transfer process between QD and TMDCs, and provide a new possibility to achieve quantum emitters on TMDCs at room

temperature by controlling the energy transfer at the single photon level.

Methods

Sample Preparation

Preparation of monodispersed QDs.

CdSe/ZnS QDs (10 mg/mL) dispersed in toluene solution (purchased from Xingzi New Material Technology Development Co., Ltd.) were first diluted 2000 times. Then we took 1 mL diluted solution and mixed it with 200 μL of 4% polymethyl methacrylate (PMMA, anisole as the solvent) by stirring at room temperature for about 1 hour to fully dissolve PMMA. Finally, to obtain monodispersed QDs, we took a 25 μL aliquot of this mixed solution and deposited it on a clean cover glass (thickness: about 170 μm) via spin-coating method at 800 revolutions per minute (rpm) for 60 s.

Preparation of QDs/MoS_2 hybrid heterostructure.

The MoS_2 monolayer and bilayer were obtained by the mechanical exfoliation from bulk materials and then transferred onto the monodispersed QD film obtained using the above-mentioned spin-coating method.

Optical Measurements

Absorption and steady-state PL measurements.

Absorption spectra of MoS_2 on transparent glass substrates were determined by a home-built transmission microscopy. A broad light beam from a tungsten halogen lamp used to illuminate our sample and the spectrum of transmitted light was recorded using a Horiba iHR320 spectrometer.

For steady-state PL, we used the 405 nm laser source (LDH-D-C-405, PicoQuant) with cw mode to excite the sample and the fluorescence signals were collected using an Olympus IX73 inverted confocal microscope with a 100× oil-immersion objective lens (NA =1.4). After filtering out the excitation laser with a 407 nm long-pass filter (LP02-407RU-25, Semrock), the steady-state PL spectrum were recorded by the spectrometer (Horiba iHR320) with a liquid-nitrogen cooled CCD (Symphony II) at ambient conditions.

Time-resolved PL measurements.

For time-resolved PL, we used the 405 nm laser with pulsed mode at a repetition rate of 40 MHz to excite the sample. The fluorescence lifetime imaging (FLIM) and PL decay curves measurements of the QDs and MoS_2 were recorded by the time-correlated single photon counting (TCSPC, HydraHarp 400 from PicoQuant) system. The QD PL emission was selected with a 575 nm band-pass filter (FF01-575/59-25, Semrock), while the MoS_2 PL emission was selected with a 660 nm band-pass filter (FF01-660/30-25, Semrock). Furthermore, PL intensity time trajectories from QD and MoS_2 were recorded by this TCSPC system.

Second-order photon correlation measurements.

The fluorescence emission from QD was sent through a 575 nm band-pass filter to a Hanbury-Brown and Twiss (HBT) setup consisting of a 50/50 beam splitter connected to two single-photon avalanche diodes (APDs, PDM Series from PicoQuant), and the second-order photon correlation function $g^2(\tau)$ was recorded by TCSPC system.

Data availability

The data that support the findings of this study are available from the corresponding author upon reasonable request.

References

1. Manzeli, S., Ovchinnikov, D., Pasquier, D., Yazyev, O. V. & Kis, A. 2D transition metal dichalcogenides. *Nat. Rev. Mater.* **2**, 17033 (2017).
2. Mak, K. F. & Shan, J. Photonics and optoelectronics of 2D semiconductor transition metal dichalcogenides. *Nat. Photonics* **10**, 216-226 (2016).
3. Xia, F. N., Wang, H., Xiao, D., Dubey, M. & Ramasubramaniam, A. Two-dimensional material nanophotonics. *Nat. Photonics* **8**, 899-907 (2014).
4. Wang, Q. H., Kalantar-Zadeh, K., Kis, A., Coleman, J. N. & Strano, M. S. Electronics and optoelectronics of two-dimensional transition metal dichalcogenides. *Nat. Nanotechnol.* **7**, 699-712 (2012).
5. Mak, K. F., Lee, C., Hone, J., Shan, J. & Heinz, T. F. Atomically thin MoS(2): a new direct-gap semiconductor. *Phys. Rev. Lett.* **105**, 136805 (2010).
6. Pospischil, A., Furchi, M. M. & Mueller, T. Solar-energy conversion and light emission in an atomic monolayer p-n diode. *Nat. Nanotechnol.* **9**, 257-261 (2014).
7. Ross, J. S. *et al.* Electrically tunable excitonic light-emitting diodes based on monolayer WSe2 p-n junctions. *Nat. Nanotechnol.* **9**, 268-272 (2014).
8. Lopez-Sanchez, O., Lembke, D., Kayci, M., Radenovic, A. & Kis, A. Ultrasensitive photodetectors based on monolayer MoS2. *Nat. Nanotechnol.* **8**, 497-501 (2013).
9. Koppens, F. H. L. *et al.* Photodetectors based on graphene, other two-dimensional materials and hybrid systems. *Nat. Nanotechnol.* **9**, 780-793 (2014).
10. Long, M. S., Wang, P., Fang, H. H. & Hu, W. D. Progress, Challenges, and Opportunities for 2D Material Based Photodetectors. *Adv. Funct. Mater.* **29**, 1803807 (2019).
11. Peng, B., Ang, P. K. & Loh, K. P. Two-dimensional dichalcogenides for light-harvesting applications. *Nano Today* **10**, 128-137 (2015).
12. Xia, F., Wang, H., Xiao, D., Dubey, M. & Ramasubramaniam, A. Two-dimensional material nanophotonics. *Nat. Photonics* **8**, 899-907 (2014).
13. Xu, M. S., Liang, T., Shi, M. M. & Chen, H. Z. Graphene-Like Two-Dimensional Materials. *Chem. Rev.* **113**, 3766-3798 (2013).
14. Ramasubramaniam, A., Naveh, D. & Towe, E. Tunable band gaps in bilayer transition-metal dichalcogenides. *Phys. Rev. B* **84**, 205325 (2011).
15. Geim, A. K. & Grigorieva, I. V. Van der Waals heterostructures. *Nature* **499**, 419-425 (2013).
16. Liu, Y. *et al.* Van der Waals heterostructures and devices. *Nat. Rev. Mater.* **1**, 16042 (2016).
17. Jariwala, D., Marks, T. J. & Hersam, M. C. Mixed-dimensional van der Waals heterostructures. *Nat. Mater.* **16**, 170-181 (2017).
18. Movva, H. C. P. *et al.* Density-Dependent Quantum Hall States and Zeeman Splitting in Monolayer and Bilayer WSe2. *Phys. Rev. Lett.* **118**, 247701 (2017).
19. Onga, M., Zhang, Y. J., Ideue, T. & Iwasa, Y. Exciton Hall effect in monolayer MoS2. *Nat. Mater.* **16**, 1193-1197 (2017).
20. Lin, K. Q., Bange, S. & Lupton, J. M. Quantum interference in second-harmonic generation from monolayer WSe2. *Nat. Phys.* **15**, 242-246 (2019).
21. Liu, X. & Hersam, M. C. 2D materials for quantum information science. *Nat. Rev. Mater.* **4**, 669-684 (2019).
22. He, Y. M. *et al.* Single quantum emitters in monolayer semiconductors. *Nat. Nanotechnol.* **10**,

497-502 (2015).
23. Koperski, M. *et al.* Single photon emitters in exfoliated WSe2 structures. *Nat. Nanotechnol.* **10**, 503-506 (2015).
24. Srivastava, A. *et al.* Optically active quantum dots in monolayer WSe2. *Nat. Nanotechnol.* **10**, 491-496 (2015).
25. Shepard, G. D. *et al.* Nanobubble induced formation of quantum emitters in monolayer semiconductors. *2D Mater.* **4**, 021019 (2017).
26. Iff, O. *et al.* Strain-Tunable Single Photon Sources in WSe2 Monolayers. *Nano Lett.* **19**, 6931-6936 (2019).
27. Peng, L. *et al.* Creation of Single-Photon Emitters in WSe2 Monolayers Using Nanometer-Sized Gold Tips. *Nano Lett.* **20**, 5866-5872 (2020).
28. Palacios-Berraquero, C. *et al.* Large-scale quantum-emitter arrays in atomically thin semiconductors. *Nat. Commun.* **8**, 15093 (2017).
29. Branny, A., Kumar, S., Proux, R. & Gerardot, B. D. Deterministic strain-induced arrays of quantum emitters in a two-dimensional semiconductor. *Nat. Commun.* **8**, 15053 (2017).
30. Xu, W. *et al.* Correlated fluorescence blinking in two-dimensional semiconductor heterostructures. *Nature* **541**, 62-67 (2017).
31. Baek, H. *et al.* Highly energy-tunable quantum light from moire-trapped excitons. *Sci. Adv.* **6**, eaba8526 (2020).
32. Hong, H. *et al.* Giant enhancement of optical nonlinearity in two-dimensional materials by multiphoton-excitation resonance energy transfer from quantum dots. *Nat. Photonics* **15**, 510-515 (2021).
33. Utzat, H. *et al.* Coherent single-photon emission from colloidal lead halide perovskite quantum dots. *Science* **363**, 1068-1072 (2019).
34. Lounis, B. & Moerner, W. E. Single photons on demand from a single molecule at room temperature. *Nature* **407**, 491-493 (2000).
35. Michler, P. *et al.* Quantum correlation among photons from a single quantum dot at room temperature. *Nature* **406**, 968-970 (2000).
36. Michler, P. *et al.* A quantum dot single-photon turnstile device. *Science* **290**, 2282-2285 (2000).
37. Goodfellow, K. M. *et al.* Distance-dependent energy transfer between CdSe/CdS quantum dots and a two-dimensional semiconductor. *Appl. Phys. Lett.* **108**, 021101 (2016).
38. Sampat, S. *et al.* Exciton and Trion Energy Transfer from Giant Semiconductor Nanocrystals to MoS2 Monolayers. *ACS Photonics* **3**, 708-715 (2016).
39. He, W. *et al.* In situ manipulation of fluorescence resonance energy transfer between quantum dots and monolayer graphene oxide by laser irradiation. *Nanoscale* **11**, 1236-1244 (2019).
40. Erdem, O. *et al.* Orientation-Controlled Nonradiative Energy Transfer to Colloidal Nanoplatelets: Engineering Dipole Orientation Factor. *Nano Lett.* **19**, 4297-4305 (2019).
41. Prins, F., Goodman, A. J. & Tisdale, W. A. Reduced dielectric screening and enhanced energy transfer in single- and few-layer MoS2. *Nano Lett.* **14**, 6087-6091 (2014).
42. Raja, A. *et al.* Energy Transfer from Quantum Dots to Graphene and MoS2: The Role of Absorption and Screening in Two-Dimensional Materials. *Nano Lett.* **16**, 2328-2333 (2016).
43. Prasai, D. *et al.* Electrical Control of near-Field Energy Transfer between Quantum Dots and Two-Dimensional Semiconductors. *Nano Lett.* **15**, 4374-4380 (2015).
44. Tanoh, A. O. A. *et al.* Directed Energy Transfer from Monolayer WS2 to Near-Infrared Emitting

PbS-CdS Quantum Dots. *ACS Nano* **14**, 15374-15384 (2020).
45. Li, C. *et al.* Resonant energy transfer between hexagonal boron nitride quantum emitters and atomically layered transition metal dichalcogenides. *2D Mater.* **7**, 045015 (2020).
46. Lounis, B. & Orrit, M. Single-photon sources. *Rep. Prog. Phys.* **68**, 1129-1179 (2005).
47. Guzelturk, B. & Demir, H. V. Near-Field Energy Transfer Using Nanoemitters For Optoelectronics. *Adv. Funct. Mater.* **26**, 8158-8177 (2016).

Acknowledgements

This work was supported by the National Natural Science Foundation of China (52022029, 91850116, 51772084, U19A2090) and the Key Program of the Hunan Provincial Science and Technology Department (2019XK2001).

Author information

Affiliations

School of Physics and Electronics, Hunan University, Changsha, 410082, China

Mai He, Cuihuan Ge, Lanyu Huang, Hepeng Zhao & Xiao Wang

Key Laboratory for Micro-Nano Physics and Technology of Hunan Province, College of Materials Science and Engineering, Hunan University, Changsha, 410082, China

Xin Yang & Anlian Pan

Institute of Physical and Theoretical Chemistry and LISA+, University of Tübingen, Auf der Morgenstelle 18, 72076, Tübingen, Germany

Kai Braun & Alfred J. Meixner

Author Contributions

X.W. conceived the original idea. M. H. performed all experiments with assistance from K.B., X. Y. and H. Z. L. H. and C. G. prepared the samples for the experiments. X. W. and M. H. analyzed the experimental data and wrote the manuscript with inputs from A.M. and A. P. X.W. and A.P. supervised the work. All authors contributed to the

discussion of results and commented on the manuscript.

Corresponding authors

Correspondence to Xiao Wang or Anlian Pan.

Ethics declarations

Competing interests

The authors declare no competing interests.

Supplementary Files

This is a list of supplementary files associated with this preprint. Click to download.

- GXXXXXXMoS2QDnaturecommunicationSupplymentaryinformationnaturecommunications.pdf